



Swansea University
Prifysgol Abertawe



Cronfa - Swansea University Open Access Repository

This is an author produced version of a paper published in:
Applied Physics Letters

Cronfa URL for this paper:
<http://cronfa.swan.ac.uk/Record/cronfa50887>

Paper:

Li, S., Wang, C. & Nithiarasu, P. (2019). Simulations on an undamped electromechanical vibration of microtubules in cytosol. *Applied Physics Letters*, 114(25), 253702
<http://dx.doi.org/10.1063/1.5097204>

This item is brought to you by Swansea University. Any person downloading material is agreeing to abide by the terms of the repository licence. Copies of full text items may be used or reproduced in any format or medium, without prior permission for personal research or study, educational or non-commercial purposes only. The copyright for any work remains with the original author unless otherwise specified. The full-text must not be sold in any format or medium without the formal permission of the copyright holder.

Permission for multiple reproductions should be obtained from the original author.

Authors are personally responsible for adhering to copyright and publisher restrictions when uploading content to the repository.

<http://www.swansea.ac.uk/library/researchsupport/ris-support/>

Simulations on an undamped electromechanical vibration of microtubules in cytosol

Cite as: Appl. Phys. Lett. **114**, 253702 (2019); <https://doi.org/10.1063/1.5097204>
 Submitted: 23 March 2019 . Accepted: 11 June 2019 . Published Online: 24 June 2019

Si Li , Chengyuan Wang , and Perumal Nithiarasu 



View Online



Export Citation



CrossMark

ARTICLES YOU MAY BE INTERESTED IN

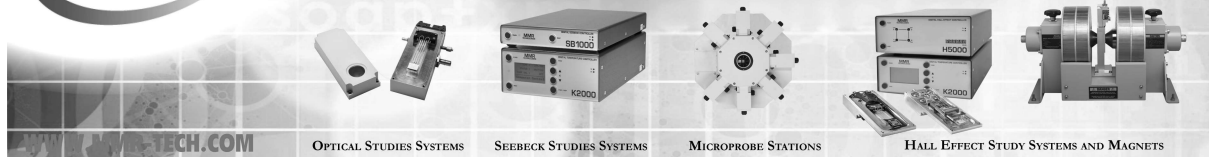
Optical and electrical properties of two-dimensional palladium diselenide
 Applied Physics Letters **114**, 253102 (2019); <https://doi.org/10.1063/1.5097825>

Substrate stiffness affects particle distribution pattern in a drying suspension droplet
 Applied Physics Letters **114**, 253701 (2019); <https://doi.org/10.1063/1.5097620>

Wurtzite phonons and the mobility of a GaN/AlN 2D hole gas
 Applied Physics Letters **114**, 253501 (2019); <https://doi.org/10.1063/1.5099957>



**THE WORLD'S RESOURCE FOR
 VARIABLE TEMPERATURE
 SOLID STATE CHARACTERIZATION**



Simulations on an undamped electromechanical vibration of microtubules in cytosol

Cite as: Appl. Phys. Lett. **114**, 253702 (2019); doi:10.1063/1.5097204

Submitted: 23 March 2019 · Accepted: 11 June 2019 ·

Published Online: 24 June 2019



View Online



Export Citation



CrossMark

Si Li,  Chengyuan Wang, ^{a)}  and Perumal Nithiarasu 

AFFILIATIONS

Zienkiewicz Centre for Computational Engineering, College of Engineering, Swansea University, Bay Campus, Fabian Way, Swansea, Wales SA1 8EN, United Kingdom

^{a)} Author to whom correspondence should be addressed: chengyuan.wang@swansea.ac.uk

ABSTRACT

This letter aims to study the electromechanical vibration of microtubules submerged in cytosol. The microtubule-cytosol interface is established in molecular dynamics simulations, and the electrically excited vibrations of microtubules in cytosol are studied based on a molecular mechanics model. The simulations show that the solid-liquid interface with a nanoscale gap significantly reduces the viscous damping of cytosol on microtubule vibration. Specifically, as far as the radial breathing modes are concerned, cytosol behaves nearly as a rigid body and thus has a very small damping effect on the radial breathing mode of microtubules. This distinctive feature of the radial breathing modes arises from its extremely small amplitude ($<0.1 \text{ \AA}$), and the relatively large gap between microtubules and cytosol (2.5 \AA) is due to the van der Waals interaction. Such a nearly undamped megahertz microtubule vibration excited by an electrical magnetic field may play an important role in designing microtubule-based biosensors, developing novel treatments of diseases, and facilitating signal transduction in cells.

Published under license by AIP Publishing. <https://doi.org/10.1063/1.5097204>

Microtubules (MTs) are one of the essential components responsible for the structural and spatial organization of eukaryotic cells.¹ They play a critical role in providing cell stiffness and facilitating cell division, migration, and self-contraction.^{2–5} MTs are constructed by protofilaments (PFs)^{6,7} comprising α - β -dimers with unbalanced charge.^{8,9} Lateral contacts of PFs contribute to more stable, rigid, and structurally intact MTs.⁶ Polarized MTs vibrate under an alternating electric field^{10,11} with the frequency up to gigahertz¹² and the amplitude around 0.1 nm .¹¹ The sensitivity of MT vibration to structural or property changes opens a door to MT-based biosensors in disease diagnostics and therapies.^{12,13}

In spite of the great potential of vibrating MTs,^{12,13} it is argued that cytosol damping in cells would quench the vibration when a non-slip solid-liquid interface (see the details in the supplementary material) is assumed for the MT-cytosol system.^{13–16} In other words, MT vibrations can survive in cells only when the cytosol damping is largely reduced by the nanoscale MT-cytosol interface due to, e.g., a slipping ionic layer near the MT surface.^{13,16,17} In addition, the solid-liquid interface at the nanoscale is found to be different from its macroscopic counterpart as the van der Waals (vdW) interaction at the interface is significant due to the largely increased surface area-to-volume ratio. It was reported in experiments that a carbon nanotube (CNT)

submerged in water can still vibrate in radial breathing modes with frequency raised by the vdW interaction between CNT and water.^{18,19} For similar reasons, a gap may exist between nanoscale MTs and cytosol due to the repulsive vdW force, which would largely decrease the cytosol damping on MT vibration. Indeed, the megahertz mechanical vibration of MTs was already detected in the wet and noisy subcellular environment of neuronal cells.²⁰ Motivated by this idea, this letter aims to investigate the MT-cytosol interface by considering the vdW force and the static electrical force at the interface and examine the influence of such an interface on the cytosol damping of MT vibration. Indeed, the unique features of the nanoscale solid-liquid interface and its effect on the dynamic behavior of MTs are a major topic of great interest in current research of nano- and biomechanics.

In this letter, the effect of the interface on the electrically excited vibration of MTs in cytosol (80% water²¹) was investigated. Molecular dynamics simulations (MDSs) were employed to study the interface between MT and water. The obtained properties were then entered into a molecular structural mechanics (MSM) model of MTs with updated values of force constants^{1,2} to examine the effect of the MT-cytosol interface on the collective vibration of MTs. The MT vibration in the present study was excited by an alternating electric field from a dipole antenna (Fig. 1).

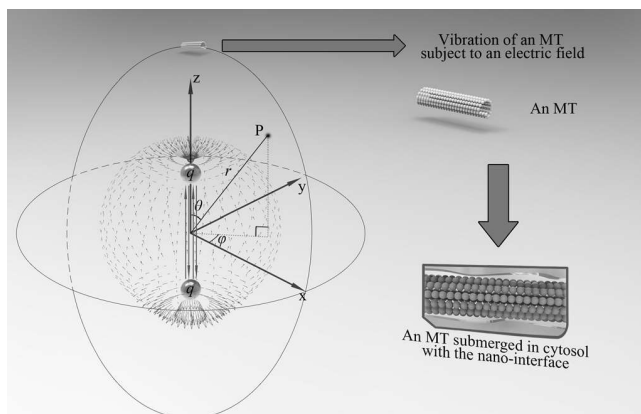


FIG. 1. Illustration of an individual MT and an MT-cytosol system subject to an electric field generated by a dipole antenna.

Herein, the MDSs were performed for obtaining an equilibrated tubulin-water system which could mimic the liquid environment (i.e., cell cytosol) surrounding MTs (see the details in the supplementary material). In the equilibrated system [Fig. 2(a)], a gap was found at the tubulin-water interface. The size of the gap, i.e., the distances to water, was measured for dimer atoms in the central rectangular region shown in Fig. 2(b). The four sides of the rectangle are 1.2 nm (the cut-off distance for nonbond interaction)^{22,23} away from the corresponding boundaries of the simulation box. The boundary effect on the interface interaction is thus eliminated. Figure 2(c) shows the histogram of the distance between water and dimer atoms where the average value d_{eq} 2.494 Å is obtained. Subsequently, to simulate the interaction potential between water molecules and the dimer [Fig. 2(d)], the water block

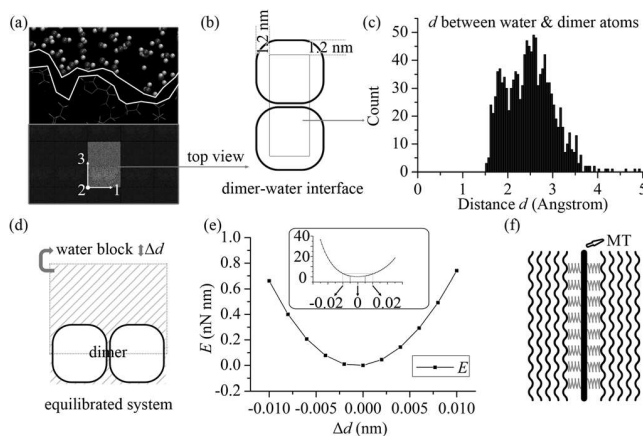


FIG. 2. (a) The illustration of the interface between MT and cytosol (inset: simulation box); (b) the dimer region within which the distance between water molecules and dimer atoms is measured; (c) the histogram of the distances measured between the dimer and water atoms; (d) the simulations on the relation between the water-dimer distance and their interaction potential energy; (e) interface potential energy E calculated as a function of the water-dimer distance change Δd ; and (f) the physical model for the nanoscale interface between MT and cytosol (case 3).

consisting of the water molecules on the upper half of the simulation box is manually moved up/down, while the dimer is fixed at its original position. The MDS was performed to acquire the interface potential energy (E) as a function of the change in the distance (Δd) between the dimer and the water block, which is measured by the distance that the water block moves [Fig. 2(d)]. It is well-known that the viscous damping significantly reduces the MT vibration amplitude in cytosol.^{14,16,24,25} A parametric study²⁴ further demonstrates that even with a largely reduced damping force due to the nanoscale interface, the amplitude of MT vibration is only on the order of 0.01 nm. Thus, in the present study, $\Delta d = 0.01$ nm was chosen in the present simulation. It can be seen that the energy-distance relation is best described by a 2nd order polynomial at $\Delta d < 0.01$ nm [Fig. 2(e)] or even larger deformation $\Delta d < 0.02$ nm [the inset of Fig. 2(e)]. Thus, the linear model $F_{nonbond} = -\partial E / \partial d \approx -k_{eq} \times (\Delta d)$ ($k_{eq} = 6999$ nN/nm) is adequate for the interaction between the dimer (or MT) and surrounding water.

In the MSM model, an MT is considered as a framed structure of beam elements which represent the protein interactions. The beam stiffnesses are calculated based on the force constants of monomeric interactions obtained in MDS.^{1,2,26,27} In addition, in modeling MT-cytosol interaction by using the MSM, an equivalent spring is used in modeling protein-water molecular interaction, where the elastic constant is measured by MDS [Fig. 2(f)] (see the supplementary material). The spring represents the nanoscale MT-water interface (supplementary material) with the equivalent thickness (i.e., the natural length of the spring) of 0.2494 nm. The damping effect of the surrounding cytosol [Fig. 2(f)] was evaluated by the damping force F_d ^{28,29} (supplementary material). In what follows, three different scenarios were considered: case (1), an MT without the surrounding cytosol; case (2), an MT-cytosol system with a nonslip solid-liquid interface, i.e., they are in physical contact and there are no gap and no relative sliding/twisting at the MT-water interface; and case (3), an MT-cytosol system with a nanoscale MT-water interface where they are separated by a small gap and coupled with the nonbond interaction modeled as a linear spring. As a result, there might be sliding or twisting relative to each other at the interface. The vibrations were then excited for the MTs by an electric field generated by a dipole antenna (see the supplementary material for the demonstrated working mechanism of the antenna-MT system).

Figure 3(a) shows that when subjected to a transverse electrical field (TEF), individual MTs [case (1)] exhibit resonant transverse vibrations at frequencies of 18.4 MHz and 78.9 MHz. The results for MTs submerged in cytosol [i.e., cases (2) and (3)] are shown in Fig. 3(b) where the damping effect of cytosol is of major concern.^{14–17} It is noted that, due to the damping effect, the amplitude decreased monotonically with the increasing frequency, at least an order of magnitude lower than those of individual MTs [Fig. 3(a)].

In the present study, the primary goal is to examine the effect of the nanoscale MT-water interface on the vibrations of MTs in cytosol, i.e., the difference between cases (2) and (3). The frequency of transverse mode II in Fig. 3(b) is found to increase from 1.099 MHz for case (2) to 2.188 MHz for case (3). A similar trend is also observed for mode III in Fig. 3(b). In addition, at a given frequency, the amplitude growth of case (3) relative to case (2) ranges from 26.1% to 146.5% in the frequency range [1 MHz, 100 MHz]. It follows that the nanoscale interface [case (3)] upshifts the frequency of the transverse vibration

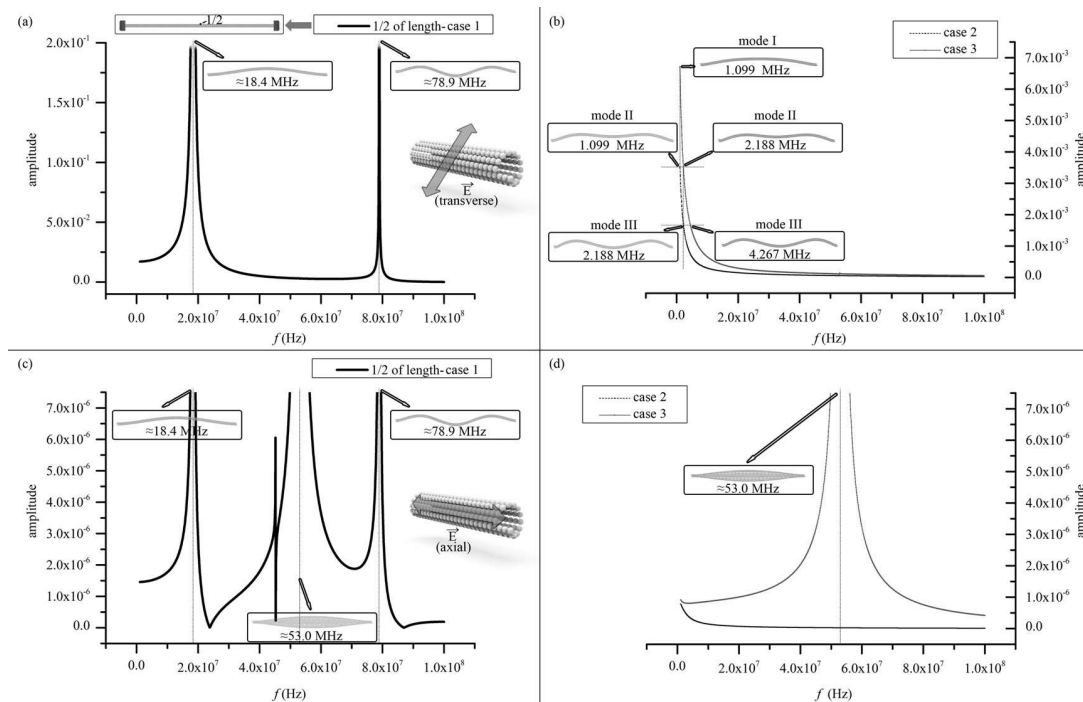


FIG. 3. The amplitude-frequency spectrum of (a) individual MT (case 1) subject to a TEF, (b) MT-cytosol system subject to a TEF with a nonslip [case (2)] or a nanoscale interface [case (3)], (c) individual MT subject to an AEF, and (d) MT-cytosol system subject to an AEF with a nonslip [case (2)] or a nanoscale interface [case (3)].

and raises the vibration amplitude at a given frequency. These can be attributed to the presence of the nanoscale interface, where the slip boundary or the gap between MT and cytosol will largely decrease the energy dissipation caused by the cytosol damping.

Figure 3(c) shows the spectrum of MT vibration [case (1)] excited by an axial electric field (AEF). It is found that an AEF generates so-called radial breathing vibration (RBV) of an MT with the associated frequency around 53 MHz. In RBV, the α and β tubulins of the MT oscillate in the radial direction as if the MT was breathing. In an MT cross section, the time-dependent change in the radius (i.e., radial vibration displacement) is equal in all directions and its amplitude [Fig. 3(c)] is found to be 3 orders of magnitudes smaller than those of transverse MT vibrations. The vibration spectra of RBV were calculated and are shown in Fig. 3(d) for the MT-water system with the nanoscale interface [case (3)] in comparison with those for the nonslip interface [case (2)]. In case (2), the vibration amplitude decreases continuously with the increasing frequency. This behavior is analogous to the transverse vibration of MTs in cytosol [Fig. 3(b)] and the vibration of a bulk solid object submerged in water. In sharp contrast, the frequency spectrum in case (3) showed a resonant vibration where the amplitude rose suddenly when the frequency approached 53 MHz, i.e., the resonant RBV frequency. This is also observed in the spectrum of the free RBV [case (1) in Fig. 3(c)]. These results indicate that the nanoscale interface can largely decrease the cytosol damping and lead to the resonant RBV of MT in cytosol [Fig. 3(d)-case (3)].

To further examine the effect of the nanoscale interface gap, we examined the trend of the amplitude with the change in the time (at a given frequency) for the MTs in all three cases considered. The forced

MT vibration was excited by an electric field and lasted for 9.75 periods (T) (i.e., stage I). Subsequently, the excitation was removed and the MT vibrated freely (i.e., stage II) in cytosol. The time-dependent amplitude at the two stages is presented in Fig. 4 with three excitation frequencies, i.e., 1 MHz, 18 MHz (i.e., the resonant transverse vibration frequency), and 53 MHz (the resonant RBV frequency). It is noted in Fig. 4(a), achieved by applying the TEF of 1 MHz, that an MT in case (1) showed nearly constant amplitudes at both stages I and II and the amplitude at stage I is found to be around 2 times greater than the one at stage II. When the cytosol was introduced, the MT of case (2) vibrated steadily at stage I, but the vibration was extinguished very quickly at stage II [Fig. 4(a)]. The trend obtained for the MT in case (3) is close to that of the MT in case (2). The difference is that, in case (3), the MT showed a greater amplitude at stage I due to the reduced damping effect in the presence of the nanoscale interface gap. For the transverse vibration at a resonant frequency of 18 MHz, the amplitude achieved in Fig. 4(b) for MTs in case (1) grew constantly at stage I and finally reached its maximum value, which remained unchanged throughout stage II. The inset of Fig. 4(b) shows how the amplitude of MTs changed in cases (2) and (3), which were similar to those shown in Fig. 4(a). These results indicated that free transverse MT vibration cannot survive the cytosol damping even if the nanoscale interface gap [in case (3)] is considered.

Next, the RBV of MTs excited by AEF was studied and is shown in Figs. 4(c) and 4(d), obtained at the frequency of 1 MHz and the resonant frequency of 53 MHz, respectively. It is noted in the two figures that, at the two frequencies, RBV was again quenched by cytosol (i.e., the amplitude faded away in a short period of time) at stage II when

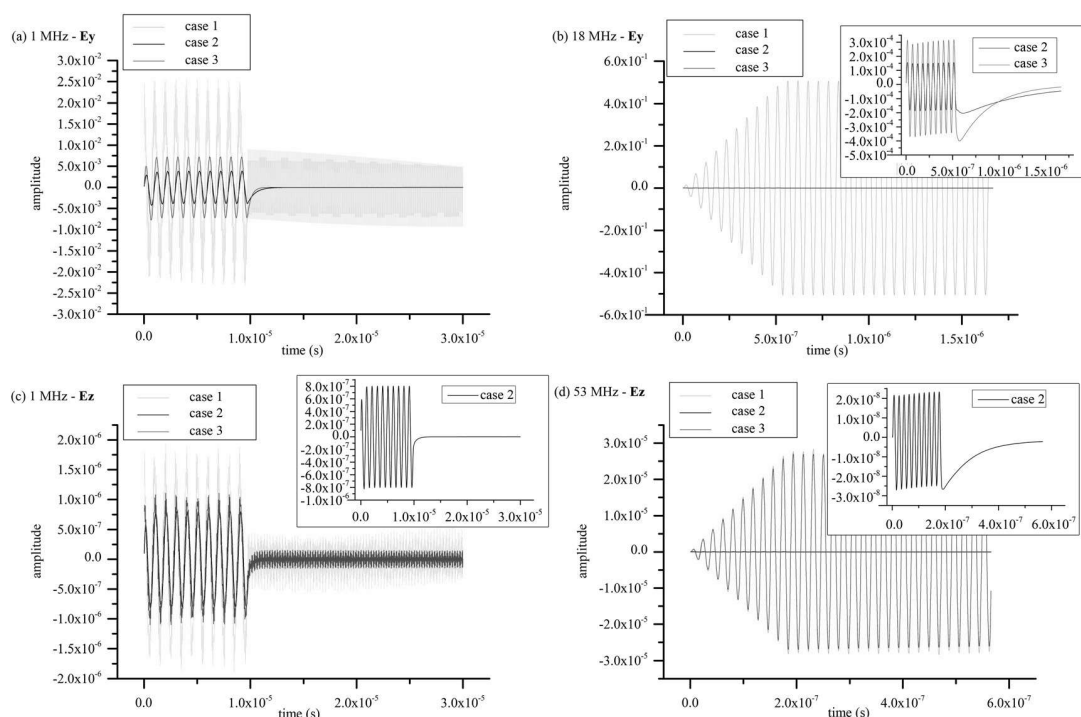


FIG. 4. Time-dependent amplitude of MT vibration excited by a TEF at frequencies of (a) 1 MHz and (b) 18 MHz and the vibration stimulated by an AEF at (c) 1 MHz and (d) 53 MHz.

the nonslip solid-liquid interface [case (2)] was assumed [the insets of Figs. 4(c) and 4(d)]. Nevertheless, when the nanoscale MT-water interface gap was introduced [i.e., case (3)], the amplitude of MT remained nearly constant or almost undamped at stage II [Figs. 4(c) and 4(d)], which was very close to the behavior of free RBV in case (1). At 1 MHz [Fig. 4(c)], the amplitude in case (3) was smaller than the one in case (1) while, at a resonant frequency of 53 MHz [Fig. 4(d)], the amplitudes in the two cases are nearly the same. Moreover, it is worth mentioning that there exists a limitation for the amplitude amplification at a value about 10 times greater than the current maximum during the prolonged AEF excitation test at 53 MHz in case (3). Based on the results, we came to the conclusion that the influence of the nanoscale MT-water interface gap is so great that it can almost eliminate the effect of cytosol damping on the RBV of MT. Such an influence turned out to be even stronger for the resonant RBV of the MT submerged in cytosol. The RBV of the MT with a high frequency and small amplitude (i.e., $<0.1 \text{ \AA}$, which is more than 1000 times smaller than those in TEF) thus is under the protection of the nanoscale solid-liquid interface gap and is promising for developing MT-based biosensors in cells. In this case, there exists the conversion between the potential energy of the nanoscale interface gap and kinetic energy of oscillating MT, but the total energy is nearly conserved with almost no energy dissipation via the motion of surrounding water. This can be attributed to the fact that due to the small amplitude of RBV, the force on the surrounding water from the oscillating MT is not large enough to generate the radial motion of the water. In other words, the water behaves like a rigid body with almost zero displacement and velocity.

Accordingly, cytosol damping or the energy dissipation via cytosol is negligible.

In summary, molecular dynamics and molecular structural mechanics simulations were performed to study the effect of the interface on the electrically excited vibration of microtubules in cytosol. It is found that a forced transverse vibration of microtubules can be excited by a transverse electrical field whose amplitude decreases with the increasing excitation frequency. The nonbond interaction between microtubules and cytosol significantly raises the frequency of a vibration mode and lifts the amplitude at a given frequency. It however does not give rise to a resonant transverse vibration of microtubules in cytosol. In addition, the free transverse vibration of microtubules will be wiped out very quickly by cytosol damping even if the nanoscale interface gap is considered.

Forced radial breathing vibration of microtubules can be stimulated by an axial electric field. Similar to the transverse vibration in cytosol, no resonant radial breathing vibration can be achieved when the nonslip solid-liquid interface is assumed. The nanoscale interface gap, on the other hand, largely decreases the cytosol damping and results in resonant radial breathing vibration of microtubules in cytosol. The amplitude of radial breathing vibration and thus the force acting on the surrounding cytosol due to the vibrating microtubule are not strong enough to generate the significant radial displacement or the velocity of the cytosol. Thus, during microtubule vibration, the surrounding cytosol behaves as if it were a rigid body. This finally leads to an almost undamped free radial breathing vibration of microtubules in cytosol. These results provide important guidance for the

development of inherent and biocompatible nanobiosensors based on microtubules in cells that would enable noninvasive diagnosis of disease and health monitoring of cells and tissues. Such a resonant radial breathing vibration of microtubules excited by an electrical field may also play a role in signal transduction in cells.

See the supplementary material for the details of the models and simulation methods.

S. Li acknowledges the financial support from the China Scholarship Council (CSC) and the College of Engineering, Swansea University.

REFERENCES

- ¹J. Zhang and C. Y. Wang, *Biomech. Model. Mechanobiol.* **13**(6), 1175 (2014).
- ²S. Li, C. Wang, and P. Nithiarasu, *Biomech. Model. Mechanobiol.* **17**(2), 339 (2018).
- ³J. Howard and A. A. Hyman, *Nature* **422**(6933), 753 (2003).
- ⁴T. Watanabe, J. Noritake, and K. Kaibuchi, *Trends Cell Biol.* **15**(2), 76 (2005).
- ⁵M. S. Kolodney and E. L. Elson, *Proc. Natl. Acad. Sci.* **92**(22), 10252 (1995).
- ⁶P. Meurer-Grob, J. Kasparian, and R. H. Wade, *Biochemistry* **40**(27), 8000 (2001).
- ⁷U. Raviv, T. Nguyen, R. Ghafouri, D. J. Needleman, Y. Li, H. P. Miller, L. Wilson, R. F. Bruinsma, and C. R. Safinya, *Biophys. J.* **92**(1), 278 (2007).
- ⁸R. Stracke, K. Böhm, L. Wollweber, J. Tuszynski, and E. Unger, *Biochem. Biophys. Res. Commun.* **293**(1), 602 (2002).
- ⁹E. Nogales, S. G. Wolf, and K. H. Downing, *Nature* **391**(6663), 199 (1998).
- ¹⁰R. Pizzi, G. Strini, S. Fiorentini, V. Pappalardo, and M. Pregolato, in *Artificial Neural Networks Engineering Tools, Techniques and Tables Mathematics Research Developments Series*, edited by S. J. Kwon (Nova Science Publishers, 2011).
- ¹¹M. Cifra, J. Pokorný, D. Havelka, and O. Kučera, *BioSystems* **100**(2), 122 (2010).
- ¹²S. Barzanjeh, V. Salari, J. Tuszynski, M. Cifra, and C. Simon, *Phys. Rev. E* **96**(1), 012404 (2017).
- ¹³J. Pokorný, C. Vedruccio, M. Cifra, and O. Kučera, *Eur. Biophys. J.* **40**(6), 747 (2011).
- ¹⁴O. Kučera, D. Havelka, and M. Cifra, *Wave Motion* **72**, 13 (2017).
- ¹⁵O. Krivosudský and M. Cifra, *EPL-Europhys. Lett.* **115**(4), 44003 (2016).
- ¹⁶J. Pokorný, *Electromagn. Biol. Med.* **22**(1), 15 (2003).
- ¹⁷C. Y. Wang, C. F. Li, and S. Adhikari, *J. Biomech.* **42**(9), 1270 (2009).
- ¹⁸M. Longhurst and N. Quirke, *J. Chem. Phys.* **124**(23), 234708 (2006).
- ¹⁹A. Rao, J. Chen, E. Richter, U. Schlecht, P. Eklund, R. Haddon, U. Venkateswaran, Y.-K. Kwon, and D. Tomanek, *Phys. Rev. Lett.* **86**(17), 3895 (2001).
- ²⁰S. Hameroff and R. Penrose, *Phys. Life Rev.* **11**(1), 39 (2014).
- ²¹V. A. Shepherd, *Current Topics in Developmental Biology* (Academic Press, 2006), Vol. 75, p. 171.
- ²²J. Wohlerlert and O. Edholm, *Biophys. J.* **87**(4), 2433 (2004).
- ²³C. Martens, M. Shekhar, A. J. Borysik, A. M. Lau, E. Reading, E. Tajkhorshid, P. J. Booth, and A. Politis, *Nat. Commun.* **9**(1), 4151 (2018).
- ²⁴S. Li, C. Wang, and P. Nithiarasu, *J. R. Soc., Interface* **16**(151), 20180826 (2019).
- ²⁵J. Pokorný, *Bioelectrochemistry* **63**(1), 321 (2004).
- ²⁶X. Y. Ji and X. Q. Feng, *Phys. Rev. E* **84**(3 Pt 1), 031933 (2011).
- ²⁷J. Zhang and S. Meguid, *Appl. Phys. Lett.* **105**(17), 173704 (2014).
- ²⁸H. Chang, Y. Zhang, J. Xie, Z. Zhou, and W. Yuan, *J. Microelectromech. Syst.* **19**(2), 282 (2010).
- ²⁹Y. H. Cho, B. M. Kwak, A. P. Pisano, and R. T. Howe, *Sens. Actuators, A* **40**(1), 31 (1994).